

ANALYSIS OF COMPARTMENTATION OF ATP IN SKELETAL AND CARDIAC MUSCLE USING ^{31}P NUCLEAR MAGNETIC RESONANCE SATURATION TRANSFER

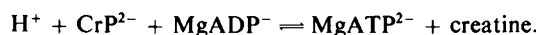
RAPHAEL ZAHLER,* JOHN A. BITTL,[‡] AND JOANNE S. INGWALL[‡]

*Section of Cardiology, Yale University School of Medicine; and [‡]Nuclear Magnetic Resonance Laboratory, Harvard Medical School and Department of Medicine, Brigham and Women's Hospital Boston, Massachusetts 02115

ABSTRACT We have developed a model for the analysis of the forward creatine kinase reaction in muscle as measured by the nuclear magnetic resonance (NMR) technique of magnetization transfer. The model, accounting for the double-exponential behavior observed in some NMR magnetization transfer data, allows for the existence of two ATP pools, one that is NMR-visible (NMR-VIS) and another that is NMR-invisible (NMR-INVIS). We have applied the model to experimental data for the forward creatine kinase reaction in skeletal and cardiac muscles to study the dependence of the creatine kinase rate constants and fluxes on workload and to account for the differences between heart and skeletal muscle. The results suggest that an NMR-distinct ATP pool exists in both heart and skeletal muscles, and that phosphate exchange with this pool catalyzed by creatine kinase increases with increased workload. The results also agree with previously published estimates of the rates of mitochondrial translocase and net ATP synthesis obtained by traditional biochemical methods.

INTRODUCTION

Creatine kinase (creatine: ATP phosphotransferase, EC 2.7.3.2.) catalyzes the transfer of a high-energy phosphate group from creatine phosphate (CrP) to ATP:



Four creatine kinase isozymes have been identified by their electrophoretic migration: BB, MB, MM and mitochondrial creatine kinase. The mitochondrial creatine-kinase isozyme is localized on the inner mitochondrial membrane (1), some of the MM isozyme is bound to the myofibril (2), the BB and MB isozymes are presumed to be cytosolic. In solution, the reaction has an equilibrium constant of ~ 166 (3).

The nuclear magnetic resonance (NMR) technique of magnetization transfer has enabled investigators to study the kinetics of this steady state reaction in intact muscle (4–11). Most investigators have analyzed ^{31}P -NMR magnetization transfer data for both the forward and reverse reactions using the 2-site chemical exchange model of Forsen and Hoffman (12). Analyzing data for the reverse creatine kinase reaction using this model is complicated by the fact that ATP is the substrate for many enzymes, including myosin ATPase, creatine kinase, and adenylate kinase. In contrast, CrP participates only in one enzymatic reaction, the creatine kinase reaction. The conversion of CrP to creatinine is thought to be nonenzymatic and slow. The fact that CrP participates in no other enzymatic

reactions simplifies the analysis of NMR magnetization transfer experiments measuring the forward creatine kinase reaction ($\text{CrP} \rightarrow [\gamma - \text{P}]\text{ATP}$).

Compartmentation of reactants can influence analysis of magnetization transfer measurements. Compartmentation of a metabolite that is NMR-visible and saturable has no effect on analysis of magnetization transfer data using the Forsen-Hoffman model of 2-site exchange (4). Some cellular pools, however, may not be NMR-visible and -saturable, which would affect analysis of magnetization transfer data. Here we develop a model to take into account a pool of NMR-invisible nonsaturable ATP (ATP-INVIS) and explore some of the consequences of such compartmentation on calculations of the forward creatine kinase flux in heart and skeletal muscle.

^{31}P -NMR magnetization transfer data from this laboratory for heart (4) and skeletal muscle preparations define the entire time course of saturation transfer, obtaining data at progressively longer durations of saturation. Using these data, the model described here is compatible with the existence of a rapidly exchanging ATP-INVIS pool in muscle. Specifically, we show that if all the cellular ATP is NMR visible and identical, the decay of the magnetization of CrP with time must be monoexponential. In contrast, our experimental data show that the decay of CrP is not always a single exponential. Therefore, the 2-site exchange model for the forward creatine kinase reaction may not be correct. Instead, these observations suggest that CrP participates in a reaction involving a substance that is NMR-

distinct from soluble ATP. If the classical assumption that CrP exchanges only with ATP is correct, then a fraction of the total cellular ATP must have different NMR properties from the soluble cytoplasmic ATP.

METHODS

The Mathematical Model: Classical Compartmental Analysis Applied to Magnetization Transfer Data

We will first show that analysis of saturation transfer experiments by the classical method of Forsen and Hoffman (12) is essentially the same mathematically as compartmental analysis, a standard tool used to study physiological and pharmacokinetic systems. The equations for exchange of a labeled substance between two biological compartments, A and C (Fig. 1 A), are

$$y_1' + ay_1 + by_2 = 0 \quad (1)$$

$$y_2' + cy_1 + dy_2 = 0, \quad (2)$$

where $y_1(t)$ = content of compartment C at time t , $y_2(t)$ = content of compartment A at time t , $y_i'(t) = dy_i/dt$, and a, b, c, d are given in terms of the pseudo-unidirectional rate constants, k , by

$$\begin{aligned} a &= k_{C \rightarrow A} + k_{C \rightarrow \text{out}} \\ b &= -k_{A \rightarrow C} \\ c &= -k_{C \rightarrow A} \\ d &= k_{A \rightarrow C} + k_{A \rightarrow \text{out}} \end{aligned}$$

The Forsen-Hoffman equations for interchange of Z-magnetization between two compartments A and C are

$$\frac{dM^C}{dt} = \frac{M^C(0)}{T_1^C} - \left[\frac{1}{T_1^C} + k_{C \rightarrow A} + k_{C \rightarrow \text{out}} \right] M^C + k_{A \rightarrow C} M^A \quad (3)$$

and

$$\frac{dM^A}{dt} = \frac{M^A(0)}{T_1^A} - \left[\frac{1}{T_1^A} + k_{A \rightarrow C} + k_{A \rightarrow \text{out}} \right] M^A + k_{C \rightarrow A} M^C. \quad (4)$$

Thus, the only mathematical difference between the two systems is the

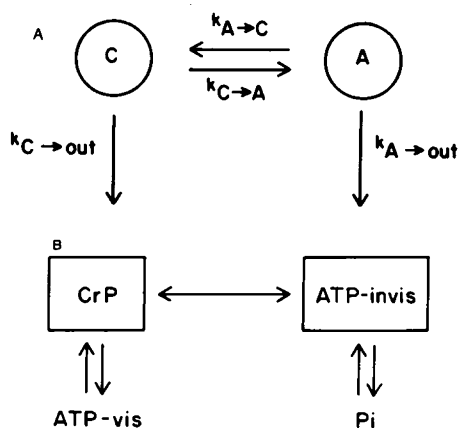


FIGURE 1. (A) Classic two-compartment system, in which we have labeled the compartments A and C. (B) Two-compartment model of the creatine kinase reaction.

presence of the constant terms

$$M^A(0)/T_1^A \quad \text{and} \quad M^C(0)/T_1^C, \quad (5)$$

and the modification of the rate constants $k_{A \rightarrow \text{out}}$ and $k_{C \rightarrow \text{out}}$ by the addition of $1/T_1^A$ and $1/T_1^C$.

The constant terms (5) convert the homogeneous system (1, 2) of coupled first-order constant-coefficient ordinary differential equations into a nonhomogeneous system (3, 4) with a constant forcing term, whose solution is easily obtained from that of the homogeneous system.

More generally, the equations of Forsen and Hoffman for the Z-magnetization in exchange reactions in systems with several nonequivalent sites A, B, C... are

$$\begin{aligned} \frac{dM^A(t)}{dt} &= [(M^A(0) - M^A(t))/T_1^A] \\ &+ \sum_{X \neq A} (k_{X \rightarrow A} M^X(t) - k_{A \rightarrow X} M^A(t)), \quad (6) \end{aligned}$$

where $M^X(t)$ is the magnetization of species X at time t , T_1^A is the spin-lattice relaxation time of species A, and the k 's are the pseudo-first-order unidirectional rate constants. Using similar reasoning, this is mathematically identical to the equations of exchange among several biological compartments A, B, C, ... with the addition of a constant term to each equation.

Application to the Creatine Kinase System when ATP Is Saturated: The Necessity of Postulating a Second ATP Pool

Fig. 2 A illustrates the primary pathways for ATP synthesis: from its metabolites and via the different creatine kinase isozymes. When $[\gamma - \text{P}] \text{ATP}$ is saturated, its magnetization is held at zero. Thus, the compartmental equations for magnetization reduce to those of a one-compartment system (Fig. 2 B). It is well known that the solution of this compartmental system is a single exponential whose rate constant is the weighted average of the rate constants of the various reactions (13). Thus, the solution of the corresponding nonhomogeneous NMR system is a single exponential plus a constant. Note that this holds despite the presence of multiple creatine kinase isozymes with different kinetic properties and does not depend on any assumptions about the values of T_1 of $[\gamma - \text{P}] \text{ATP}$ or CrP.

If, as is the case for saturation-transfer data for heart and skeletal muscle, the magnetization data for the decay of $M(t)$ are not adequately represented as a single exponential, there must be a phosphorus-containing moiety, substance X, exchanging directly with CrP that is not saturated when the gamma-peak of the NMR-visible ATP is irradiated and saturated. One candidate for this substance is a pool of ATP that is bound to a macromolecule, and thus has a broad NMR linewidth making

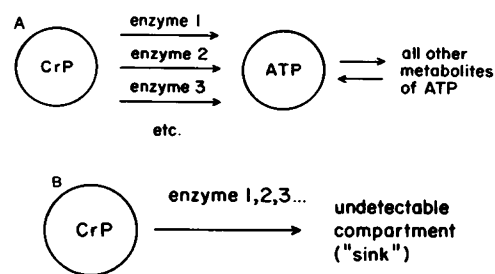


FIGURE 2. (A) Schematic diagram of ATP metabolism. Note the multiple possible creatine kinase isozymes, as well as the fact that CrP exchanges only with ATP. (B) If all ATP is saturated by an RF pulse, the system in A reduces to that shown in B.

it NMR-invisible, ATP-INVIS. Substance X could be a phosphorus-containing compound other than ATP, but this would contradict the generally accepted concept that the only compound that exchanges directly with CrP is ATP. Other nucleotides such as GTP are not good candidates. Not only are other nucleotides poor substrates for the creatine kinase reaction, but exchange with other nucleotide triphosphates in the same compartment as ATP would be indistinguishable from exchange with ATP. Note that models that assume some ATP is in a slowly exchanging but NMR-visible compartment are not compatible with the double-exponential decay of $M(t)$ (4).

The Specific Model

We now apply the general two-compartment model of Fig. 1 A to the particular system containing an ATP-INVIS pool shown in Fig. 1 B. Thus, the symbol C will now stand for CrP, and A will stand for ATP-INVIS. The rate constant, $k_{C \rightarrow A}$, in Eq. 3 is replaced by $k_{CrP \rightarrow ATP-INVIS} + [1/T_1(CrP)]$, abbreviated to $k_{C \rightarrow A} + (1/T_1^C)$; $k_{A \rightarrow C}$ in Eq. 4 is replaced by $k_{ATP-INVIS \rightarrow Pi} + [1/T_1(ATP-INVIS)]$, or $k_{A \rightarrow Pi} + 1/T_1^A$. Let $P(t)$ represent the net flux $ADP + Pi \rightarrow ATP-INVIS$ (ATP synthesis minus ATP degradation). The Forsen-Hoffman equations then become

$$y_1' + ay_1 + by_2 = e_1 \quad (7)$$

$$y_2' + cy_1 + dy_2 = e_2, \quad (8)$$

where $y_1(t) = M^C(t)$, $y_2(t) = M^A(t)$, $a-d$ are as in Eqs. 1 and 2, and

$$e_1 = \frac{M^C(0)}{T_1^C} \quad \text{and} \quad e_2 = \frac{M^A(0)}{T_1^A} + P(t).$$

We must now attempt to solve these equations to determine the rate constants.

Some of the parameters in these equations are known: we can use computer fitting techniques to derive the double-exponential function

$$M^C(t) = \alpha_0 + \alpha_1 e^{-\beta_1 t} + \alpha_2 e^{-\beta_2 t} \quad (9)$$

from our experimental data. The function $M^A(t)$, however, is unknown, since it represents the magnetization of the NMR-invisible ATP; but the total amount of this substance in the cell can be estimated. If the function $P(t)$ representing the sum of ATP synthesis and degradation is known or assumed, substituting Eq. 9 into Eqs. 7 and 8 and equating the coefficients of each exponential term yields six linear equations that we can solve for the unknowns a , b , c and d , and thence for the rate constants. This is similar to a standard procedure in pharmacokinetics for obtaining rate constants for the transfer of a drug between different compartments when the concentration-time curve of the drug in only one compartment is known.

The solution of the resulting equations depends on assuming values for: (a) T_1 of CrP, (b) T_1 of ATP-INVIS, (c) the concentration of ATP-INVIS, and (d) the function $P(t)$. The value $P(0)$ represents the steady state net flux from Pi to ATP-INVIS (where $P(0)$ is negative if the net flux is from ATP-INVIS to Pi). Values for $P(0)$ can thus be approximated from published data (4, 14). To obtain the rest of the time-dependent function $P(t)$ we can write

$$P(t) = k_{syn} M^{Pi}(t) - k_{deg} M^{ATP-INVIS}(t), \quad (10)$$

where k_{syn} is the rate constant for the reaction $ADP + Pi \rightarrow ATP-INVIS$ and k_{deg} is the rate constant for the reverse reaction.

Determining $M^{Pi}(t)$ from the experimental data is difficult since the Pi peaks are relatively small. To simplify the mathematics, we assume that the magnetization of Pi decreases with time according to a double-exponential function with the same exponents as Eq. 9:

$$M^{Pi}(t) = v M^{ATP-INVIS}(t) + w,$$

where v and w are unknown constants. Then

$$P(t) = (v k_{syn} - k_{deg}) M^{ATP-INVIS} + w k_{syn}.$$

This solution gives us the desired rate constants and fluxes between the ATP pools and CrP.

Note that there are methodologic problems in the use of nonlinear regression techniques to fit Eq. 9. Unless the slopes of the fast and slow phases of the decay differ by a factor of at least 3, there will usually be many possible double-exponential functions that fit the data equally well, making it impossible to determine the rate constants (13). The asymptotic value of the magnetization, M_∞ , is also crucial to the fit, since small changes in M_∞ may have a significant effect on the values of the other parameters.

³¹P-NMR Methods

We used this mathematical model to analyze data obtained for saturation-transfer experiments of heart and skeletal muscle. The isolated, perfused isovolumic rat heart was studied at four levels of cardiac performance and oxygen consumption as described (4). Cardiac performance, calculated as the product of heart rate and developed pressure (the difference between systolic and diastolic pressures) was 0, 15.2 ± 2.2 , 22.7 ± 1.6 , and 39.5 ± 1.9 1,000 mmHg/min for the arrested heart and at low, medium and high workload. Corresponding values for oxygen consumption were 5.9 ± 1.9 , 17.9 ± 2.3 , 25.0 ± 1.9 , and 41.0 ± 3.4 $\mu\text{mol O}_2$ g dry weight⁻¹ s⁻¹. Each scan was preceded by a low-power radio frequency pulse to saturate the $[\gamma - P]$ of ATP for time periods ranging from 0 to 4.8 s. For the skeletal muscle studies, rats were sedated and placed in an NMR probe with a 1 cm, 2-turn surface coil over the quadriceps muscle. Magnetization transfer pulse sequences with delays ranging from 0.1 to 4.8 s were employed to analyze both the resting and (electrically) stimulated states. Data are plotted as magnetization units (where 1,000 units equal 25 $\mu\text{mol/g}$ dry weight) vs. time of saturation.

Nonlinear regression (BMDP program P3R and SAS procedure

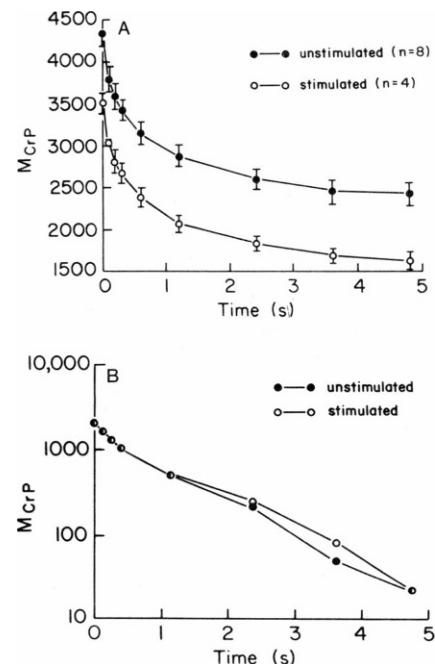


FIGURE 3. Magnetization transfer data obtained from rat quadriceps muscle preparation. (A) The raw data plotted linearly. (B) The calculated M values of 2,398 (unstimulated) and 1,598 (stimulated) have been subtracted and the data plotted on a log scale to illustrate the double-exponential behavior.

NLIN) or exponential peeling was used to fit single-exponential plus constant and double-exponential plus constant functions to the experimental data. The corresponding 3- or 5-variable fits yield M_{∞} (the coefficient α_0 in Eq. 9). Data from all experiments at a given workload were averaged and weighted by the reciprocal of the variance at each point.

Goodness of fit was assessed by the chi-square test, with one degree of freedom subtracted for each variable estimated from the input data (15, 16). This technique adjusts for the fact that increasing the number of parameters in any fitting procedure always leads to at least as good a fit.

RESULTS

For magnetization-transfer data for both the unstimulated and stimulated skeletal muscle preparations (Fig. 3), the single-exponential fit was rejected by the chi-square test for goodness of fit (unstimulated: chi square = 37.6, $df = 5$; $P < 0.0001$), while the double exponential fit was not rejected (chi square = 0.85, $0.1 < P < .25$). Similar results were obtained for unweighted data. To confirm that the single-exponential fit was inappropriate, another method was employed: a single-exponential-plus-constant function was fitted to the last four points of each curve to obtain M_{∞} , and then a 2- or 4-parameter nonlinear regression was employed to find the best single- and double-exponential fits with this fixed M_{∞} . Again, the single-exponential fits were rejected by the chi-square test.

The corresponding data for the isolated perfused rat heart (from reference 4) do not have an adequate number of points on each magnetization transfer curve to assess rigorously goodness-of-fit or perform 5-parameter fits. Double-exponential functions were fitted to the high-workload data using M values estimated by eye, followed by the method of exponential peeling. Data for the three lower heart workloads were fitted adequately with a single exponential, and the model was applied to the single-

exponential by treating it as a sum of two identical exponential terms.

Skeletal Muscle

To solve the equations describing the double-exponential function obtained from the magnetization-transfer data, four additional parameters are required as input: the T1 values of CrP and of ATP-INVIS, the initial magnetization of ATP-INVIS, and the net flux from Pi to ATP-INVIS. We denote these values by T_1^C , T_1^A , m and $P(0)$, respectively. We assume that there is no direct exchange (17) between ATP-INVIS and ATP-VIS (cytosolic ATP) so that $k(A \rightarrow \text{sat}) = 0$. Then, for fixed m and T_1^C and a given value of $P(0)$, it follows that the corresponding solution of Eqs. 5 and 6 does not depend on T_1^A . Table I presents the output of the model for selected values of the parameters T_1^C , m , and $P(0)$. We now explain the reasons for choosing the particular parameter values shown.

Previous work from our laboratory indicates that T_1^C in muscle is approximately 2.1 s regardless of workload. Values of T_1^C greater than 1.9 s make the equations impossible to solve for the unstimulated muscle unless a very large pool size m (>20% of total ATP) is assumed. There is a singularity of the equations for the unstimulated case at a T_1^C value of approximately 1.85 s. For the stimulated muscle, varying T_1^C from 1.9 to 2.7 s has little effect on the results (Table I). The results do not depend on the T1 value of the ATP-VIS pool.

The parameter m represents the size of the ATP-INVIS pool as a fraction of the total NMR-visible ATP pool, which is arbitrarily set to 1,000 magnetization units. We studied the model with m ranging from 5 to 150 magnetization units (0.5 to 15% of the total ATP pool). Values of

TABLE I
PREDICTED RATE CONSTANTS AND FLUXES FOR CREATINE KINASE REACTION FOR SKELETAL MUSCLE USING A COMPARTMENTATION MODEL

m	Workload	T_1^C	CrP \rightarrow ATP-INVIS		CrP \rightarrow ATP-VIS		ATP-INVIS \rightarrow CrP		Total flux ATP-INVIS \rightarrow ATP-VIS	Total flux CrP \rightarrow ATP
			k	Flux	k	Flux	k	Flux		
150	U	1.9	1.8	8,000	0.30	1,300	7.9	1,200	350	9,200
	S	2.7	1.0	3,400	1.2	4,200	9.3	1,400	1,700	7,600
	S	2.1	0.91	3,200	1.3	4,600	10	1,600	2,000	7,700
	S	1.9	0.89	3,100	1.3	4,700	10	1,600	2,200	7,800
100	U	1.9	1.8	7,700	0.3	1,100	7.8	780	200	8,800
	S	2.7	0.76	2,700	1.3	4,600	12	1,200	1,500	7,300
	S	2.1	0.72	2,500	1.4	4,900	13	1,300	1,800	7,500
	S	1.9	0.70	2,500	1.4	5,100	13	1,300	1,900	7,500
50	U	1.9	1.8	7,900	0.1	520	7.3	360	44	8,400
	S	2.7	0.47	1,700	1.5	5,400	18	900	1,400	7,100
	S	2.1	0.45	1,600	1.6	5,600	20	1,000	1,600	7,200
	S	1.9	0.44	1,600	1.6	5,700	20	1,000	1,700	7,200

U = unstimulated, S = stimulated; rate constants are in seconds⁻¹, fluxes in magnetization units per second. All values are rounded to first two significant digits.

m less than 50 tended to give unrealistically large values for the rate constant from ATP-INVIS to CrP.

We obtained estimates of $P(0)$ from literature values for oxygen consumption of resting mouse soleus and tetanic mouse extensor digitorum longus muscles (14). In the steady state, total ATP synthesis must equal total ATP degradation. If we assume that all the ATP-INVIS is located in the mitochondrion, then $P(0)$ will be equal to the measured rate of respiratory ATP production. On the other hand, suppose that all the ATP-INVIS is on the myosin head (the primary ATPase in muscle). In this case, ATP-INVIS degradation will equal the rate of ATP synthesis and $P(0)$ will equal the negative of the rate of ATP production. ATP-INVIS could be divided between both locations, which would yield a value of $P(0)$ somewhere between these two extremes.

For stimulated muscle, the assumption that all the ATP-INVIS lies on the myosin head results in no solution for the equations unless we assume an unrealistically large ATP-INVIS pool size (>20% of total ATP). This suggests that the data are inconsistent with the ATP-INVIS lying completely at the myosin head. For unstimulated muscle, the equations are solvable (and yield approximately the same solution) regardless of the choice of $P(0)$.

Table I presents the output of the model based on the assumption that all the ATP-INVIS is at the mitochondrion. In this case, the indirect transfer between ATP-INVIS and ATP-VIS occurs via the mitochondrial creatine kinase reaction. Total flux ATP-INVIS \rightarrow ATP-VIS is calculated by the formula $[\text{ATP-INVIS}](k_1)(k_2)$, where k_1 is the rate constant from ATP-INVIS to CrP and k_2 is the rate constant from CrP to ATP-VIS. Total flux CrP \rightarrow ATP is calculated as the sum of the fluxes CrP \rightarrow ATP-INVIS and CrP \rightarrow ATP-VIS. Results shown in Table I suggest that the flux from ATP-INVIS (in the mitochondrion) to ATP-VIS (presumably in the cytosol, at the myosin head, etc.) increases in the stimulated muscle, even though there is little change in the net flux through the creatine kinase reaction. Data shown in Table I also suggest that the increased delivery of ATP to myosin and other ATP-utilizing sites in stimulated muscle is mediated primarily by a large increase in the rate of cytosolic transfer from CrP to ATP (CrP \rightarrow ATP-VIS). The transfer of phosphate from ATP-INVIS to CrP via the mitochondrial creatine kinase reaction shows a smaller increase in flux.

In addition, the rate constants for the reaction ATP-INVIS to CrP, which range from 7.3 to 20 s⁻¹ (Table I), are in agreement with the half-time of translocase of 70 ms derived by Chance (18) for rat-liver mitochondrial membranes.

We now demonstrate that the data fit the compartmentation model better than the conventional 2-site model. The experimental data can be approximated either by the best single-exponential fit or one of the terms of the best double-exponential fit. Each method yields different flux

values; however, for a given method, flux from CrP to ATP is the same for both stimulated and unstimulated muscles (Table II). The method using only the fast term of the double-exponential fit results in a decrease in flux upon stimulation and excessively short T_1^C values. This indicates that analyzing saturation transfer by using data defining only the early part of the decay curve (at short saturation times) leads to unreasonable values and is probably incorrect.

Heart

For the isolated perfused rat heart, T_1^C is 2.1 s (4). Assuming that direct exchange between ATP-INVIS and ATP-VIS is negligible (17) compared to exchange mediated by creatine kinase, the results of the compartmentation model do not depend on T_1^A . Values of $P(0)$ were obtained from reported oxygen consumption data (4). As in the case of skeletal muscle, $P(0)$ will be positive if we assume that ATP-INVIS lies entirely at the mitochondrion or negative if it lies entirely at the myosin head.

The parameter m represents the size of the ATP-INVIS pool. Previous work indicates that ~10% or less of total cardiac ATP is in mitochondria (19). We have evaluated the model for values of m ranging from 5 to 150, corresponding to a ATP-INVIS pool of 0.5 to 15% of NMR-visible ATP. Values for the rate constants for the exchanges CrP to ATP-INVIS and CrP to ATP-VIS, as well as the flux from CrP to ATP, show little dependence on the value of m ; results for $m = 25$ magnetization units are displayed in Table III and Fig. 4. In contrast, the rate constants and the fluxes for ATP-INVIS \rightarrow CrP and for ATP-INVIS \rightarrow ATP-VIS do depend on m (Table IV and Fig. 5). The results do not indicate which value of m is most suitable. For the assumption that ATP-INVIS is at the mitochondrion, flux from CrP to ATP-INVIS is negligible for all workloads (Table III), whereas the flux for the reaction ATP-INVIS \rightarrow CrP (as well as the reaction CrP \rightarrow ATP-VIS) increases with workload (Table III and Fig. 6). This results in a net flux from mitochondrial ATP

TABLE II
COMPARISON OF METHODS OF ANALYSIS OF
MAGNETIZATION-TRANSFER DATA: CREATINE KINASE
REACTION IN SKELETAL MUSCLE

	Method	T	Rate constant	Flux
Unstim	Single	1.19	0.52	2,081
Stim		1.34	0.61	2,460
Unstim	Double, fast	0.17	4.72	20,500
Stim		0.29	4.05	14,200
Unstim	Double, slow	2.26	0.36	1,550
Stim		3.13	0.38	1,330

Rate constants are in seconds⁻¹, fluxes in magnetization units per second. Single = single-exponential fit; double, fast = fast term of double-exponential fit; double, slow = slow term of double exponential.

TABLE III
PREDICTED RATE CONSTANTS AND FLUXES FOR THE
CREATINE KINASE REACTION IN HEART AT
DIFFERENT WORKLOADS WHEN ATP-INVIS IS
2.5% OF TOTAL ATP

Workload	CrP → ATP-INVIS		CrP → ATP-VIS		ATP-INVIS → CrP		Total flux ATP-INVIS → ATP-VIS	Total flux CrP → ATP
	<i>k</i>	Flux	<i>k</i>	Flux	<i>k</i>	Flux		
For ATP-INVIS in mitochondria								
K-arrest	0	0	0.3	420	1.5	37	11	420
Low	0	0	0.8	1,200	2.8	70	59	1,200
Medium	0	0	1.1	1,400	4.7	120	120	1,400
High	0.03	34	1.7	2,000	7.2	180	300	2,000
For ATP-INVIS in myofibrils								
K-arrest	0	0	0.3	400	0.4	10	3	330
Low	—	—	—	—	—	—	—	—
Medium	—	—	—	—	—	—	—	—
High	0.6	730	0.96	1,100	0.62	16	15	1,900

Predicted rate constants (*k*) and fluxes for the creatine kinase reaction assuming a total ATP-INVIS pool of 25 magnetization units (2.5% of total cellular ATP) at four levels of cardiac performance. Cardiac performance, defined as the product of heart rate and developed pressure (i.e., the difference between systolic and diastolic pressures), was 0 for K-arrested hearts and 15, 23, and 38 × 10³ mmHg/min for low, medium, and high workload hearts, respectively. For the assumption that the ATP-INVIS is all at the mitochondrion, the equations have two possible solutions for medium-workload hearts; the solution shown correlates better with the data for other workloads. Units are seconds⁻¹ for *k* and magnetization units per second for flux. —, no solution exists.

(ATP-INVIS) to cytoplasmic ATP (ATP-VIS) that increases more than 25-fold from the arrested heart to hearts operating at maximal workload (Fig. 7). The model also predicts that net ATP synthesis (ATP-INVIS → ATP-VIS) for high workload hearts is ~1.8 μmol min⁻¹ mg mitochondrial protein⁻¹. This is in excellent agreement with the value of 1.7 ± 0.2 μmol min⁻¹ mg mitochondrial protein⁻¹ obtained by LaNoue et al. (20) from ³¹P-labeled phosphate exchange kinetics in rat-heart mitochondria.

Net flux from CrP to ATP increases fivefold over the

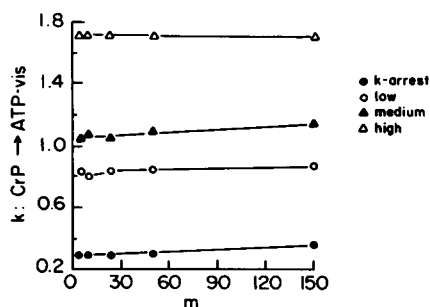


FIGURE 4. Rate constants for the reaction CrP → ATP-VIS obtained from the model for the isolated perfused heart, assuming that *m* = 25, and that ATP-INVIS is located exclusively in the mitochondria.

TABLE IV
PREDICTED RATE CONSTANTS AND FLUXES FOR THE
CREATINE KINASE REACTION IN THE
HIGH-WORKLOAD HEART FOR VARIOUS
SIZES OF THE ATP-INVIS POOL

<i>m</i>	ATP-INVIS → CrP		ATP-INVIS → ATP-VIS	
	<i>k</i>	Flux	Flux	
For ATP-INVIS in mitochondria				
5	33	160	280	
10	17	170	280	
25	7.2	180	300	
50	3.9	200	330	
150	1.7	250	430	
For ATP-INVIS in myofibrils				
5	0.64	3	3	
10	0.63	6	6	
25	0.62	16	15	
50	0.60	30	30	
150	0.54	82	86	

Units are *k*(s⁻¹) and flux (magnetization units per second).

range of cardiac performance studied (Table III). For the three lowest workloads, where a single-exponential fit describes the data satisfactorily, the compartmentation model yields values for flux from CrP to ATP which are similar to those obtained by standard methods (Fig. 7). The values are dissimilar only for high-workload hearts.

The assumption that the ATP-INVIS is all at the myosin head leads to no solution for low and medium workloads, invalidating the assumption (Table III).

DISCUSSION

A single-exponential function does not always adequately describe magnetization transfer data for heart and skeletal muscle. This observation is consistent with the existence of an NMR-distinct ATP pool. We developed a kinetic model to evaluate the consequences of an NMR-distinct ATP compartment in the myofibril or mitochondria on calculation of the forward creatine kinase flux. For both heart and stimulated skeletal muscle, the compartmentation

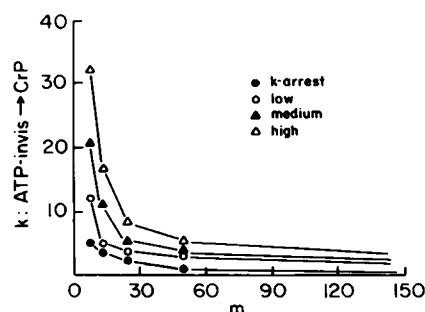


FIGURE 5. Rate constants for the reaction ATP-INVIS → CrP (same assumptions as Fig. 4).

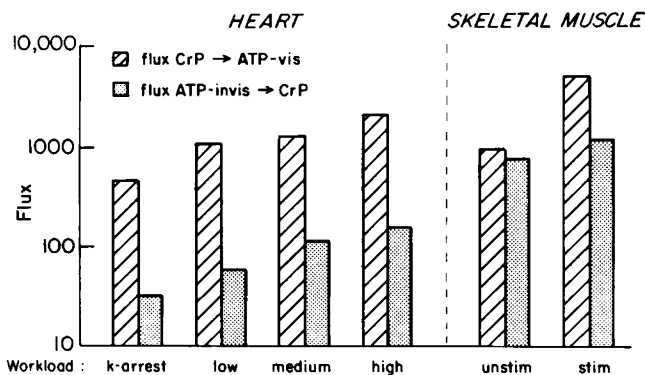


FIGURE 6. Workload dependence of fluxes in heart and skeletal muscle. Assumptions: for heart, $m = 25$, T_1 of CrP = 2.1; for muscle, $m = 100$, T_1 of CrP = 1.9.

model is consistent with localization of a NMR-distinct ATP invisible pool at mitochondria, and is inconsistent with localization exclusively in the myofibril. In addition, these results agree with previous work of LaNoue et al. and Chance (18, 20) using traditional biochemical methods.

Comparison of results derived from the compartmentation model for heart and skeletal muscle at low and high workloads are shown in Fig. 8, *A* and *B*. They can be summarized as follows: (a) Since direct exchange of ATP-INVIS and ATP-VIS is negligible (17), exchange of ATP-INVIS to ATP-VIS occurs via ATP/ADP translocase and the creatine kinase reaction. For both heart and skeletal muscle, flux from ATP-INVIS to ATP-VIS increases with increased workload. This increase is due to increased flux for both components of the exchange, ATP-INVIS → CrP and CrP → ATP-VIS. (b) For heart, flux for both ATP-INVIS → CrP and CrP → ATP-VIS increases about fivefold as cardiac performance increases from zero in the arrested heart to double products of 45,000 mmHg/min in high-workload hearts. In stimulated skeletal muscle, flux for CrP → ATP-VIS is higher than flux for ATP-INVIS → CrP. (c) Flux for the reaction CrP → ATP-INVIS is zero in heart; in skeletal muscle, this flux is nonzero and decreases with stimulation. (d)

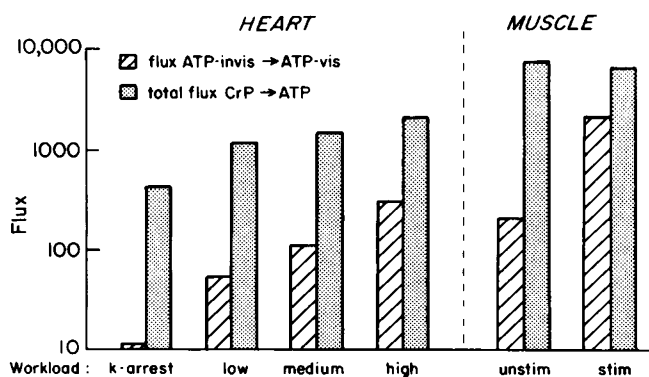


FIGURE 7. Workload dependence of derived fluxes; same assumptions as in Fig. 6.

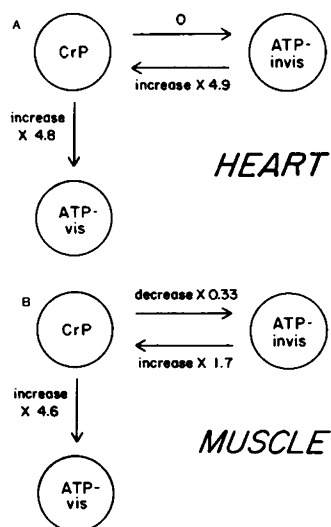


FIGURE 8. Summary of changes in flux from lowest to highest workload in heart and skeletal muscle. Assumptions as in Fig. 6.

Total creatine kinase flux (CrP → ATP) increases with workload in heart, but not in skeletal muscle.

The Role of ATP Compartmentation on Calculations of Creatine Kinase Flux

Compartmentation of phosphate metabolites is well established. Inorganic phosphate is distributed between the cytosol and mitochondria. ATP may be sequestered into several pools, including myofibrils and mitochondria. In heart, as much as 10% of total ATP is in mitochondria (19). Bittl and Ingwall (4) point out that compartmentation of a fraction of ATP in a slowly exchanging pool does not alter calculations of creatine kinase fluxes, assuming that this ATP pool is NMR-visible and saturable. The compartmentation model presented here evaluates the effect of an ATP pool that is NMR-invisible and unsaturable on calculation of flux for the forward creatine kinase reaction.

Gadian et al. (10) speculate that the ATP bound to actomyosin has a lower T_1 than cytosolic ATP, and thus its saturation would disappear before P_i was formed. If indeed the ATP-INVIS pool is nonsaturable because its T_1 is much shorter than that of cytosolic ATP, the findings of Gadian et al. (10) that T_1 of ATP varies depending on workload, while the T_1 of CrP does not, might be explained by a change in the relative amounts of saturable and nonsaturable ATP. On the other hand, NMR-invisible ATP would not be expected to have any effect on calculations of T_1 in the absence of exchange. Bittl and Ingwall (4) observed no dependence of T_1 on workload in the absence of exchange for either ATP or CrP for heart.

Using NMR magnetization transfer methods, Meyer et al. (11) found that creatine kinase flux in resting cat-biceps muscle was similar to creatine kinase flux measured in a solution containing the same specific activity of enzyme.

This could be interpreted as evidence against compartmentation in muscle. A more stringent test of compartmentation, however, is to evaluate creatine kinase flux in muscles under different physiologic conditions. Comparison of creatine kinase fluxes in vitro and in heart in vivo suggest that results obtained in solution do not mimic the in vivo situation. Kupriyanov et al. (5) have shown that changes in creatine kinase flux with increased cardiac performance cannot be mimicked by varying substrate concentrations in solutions of creatine kinase. The compartmentation model developed here is one way to analyze magnetization transfer data for creatine kinase flux in vivo.

Several groups have used magnetization-transfer NMR to study heart creatine kinase kinetics (4-9) and have interpreted the results in terms of metabolic compartmentation. ATP compartmentation has been cited as one explanation for the apparent discrepancy between the forward and reverse fluxes of the creatine kinase reaction in the beating heart (6, 9). Conversely, equality of the forward and reverse fluxes has been cited as evidence against substrate compartmentation (8). The apparent differences in results can be explained by differences in the physiological preparations: differences between the apparent forward and reverse fluxes are observable only in beating hearts operating at high workload. Although the compartmentation model developed here analyzes only the forward creatine kinase reaction and, thus, cannot address the apparent discrepancy between the forward and reverse fluxes, our analysis shows that magnetization transfer data obtained over a wide range of cardiac performance are consistent with compartmentation of ATP.

Koretsky et al. (21, 22) studied creatine kinase flux in kidney and heart in intact rats using chronically implanted radiofrequency coils. They found that two-dimensional NMR and inversion transfer techniques could not detect the effects of small metabolite pools, but that saturation transfer NMR using a continuous saturation pulse was sensitive to the presence of small metabolite pools. To explain these results, they proposed a model based on two pools of ATP, one large (cytosolic) and NMR-visible, the other (at mitochondria and myofibril) small and NMR-invisible. Their model predicts that saturation transfer measurements will yield a forward rate constant greater than the reverse rate constant, while two-dimensional NMR techniques would measure equal apparent rate constants. This analysis is helpful for reconciling apparent discrepancies between the forward and reverse fluxes through the creatine kinase reaction. Note that the compartmentation model for the forward creatine kinase reaction developed in this report explores the consequences of a different assumption, namely that the invisible ATP pool is not saturated during the course of the magnetization transfer experiment. Another difference is that the Koretsky model analyzes steady state data while our model exploits the mathematics inherent in analyzing time-

dependent saturation-transfer data. The model presented here also explains the double-exponential behavior sometimes observed for saturation-transfer data defining the forward creatine kinase reaction. Finally, our model provides a method to calculate rate constants of the component phosphate exchange reactions linking compartmental and cytosolic ATP.

The values for total creatine kinase flux ($\text{CrP} \rightarrow \text{ATP}$) of 7,100-9,200 magnetization units/s calculated here for rat skeletal muscle are about 10 times higher than values for creatine kinase flux for unstimulated isolated cat muscle reported by Kushmerick and colleagues (11). If we ignore the flux through ATP-INVIS, however, our calculations yield values for creatine kinase flux of about 520 to 1,300, which is much closer to that reported for cat muscle (11). These results suggest that analyzing NMR magnetization transfer data using a model that ignores compartmentation misses a large component of net flux through a NMR-invisible ATP pool. This analysis also suggests that the missing component is in rapid exchange. Consistent with this prediction, creatine kinase flux in rat skeletal muscle calculated using the compartmentation model presented here is six times faster than flux obtained using two-dimensional magnetization transfer methods (24) (13 vs. $70 \mu\text{mol g}^{-1}\text{s}^{-1}$). As pointed out by Balaban et al. (23) and Koretsky et al. (22) and discussed above, small pools in rapid exchange are not detected by two-dimensional magnetization-transfer methods, but should be detectable using saturation transfer techniques. The rate constants for the missing reaction, $\text{ATP-INVIS} \rightarrow \text{CrP}$, calculated by the compartmentation model presented here, are indeed high: $7-18 \text{ s}^{-1}$. They are, however, compatible with the work of Chance in rat liver mitochondria (18). These comparisons emphasize the magnitude of the contribution of flux through an NMR-invisible ATP pool on creatine kinase kinetics.

As indicated by the mathematical analysis described here, the existence of an invisible, nonsaturable metabolite pool is predicted by the double-exponential nature of the magnetization transfer experiment and was not assumed a priori. Precise identification of the identity of the ATP-INVIS pool cannot be made, however. The NMR-invisible pool could be a compound other than ATP, but, since it must exchange with CrP, this seems unlikely. ATP that was invisible because it was bound may not be a good candidate: bound ATP would be expected to have a longer T_1 than unbound ATP (in contradiction to the speculation of Gadian et al. [10] mentioned above), which would increase, not decrease, saturability. On the other hand, a substance that was invisible because it had an inhomogeneously broad linewidth would be expected to have a short T_2^* , and hence require a higher power rf pulse to be saturated. The environment of the ATP-INVIS pool could also attenuate the saturating pulse. For example, the structure or composition of the mitochondrion (e.g., ferro-

magnetic iron atoms in cytochromes) may slow the rate of ATP saturation. The mitochondrial environment might also alter the resonant frequency of the mitochondrial ATP pool enough so that it would not be saturated by a pulse set at the frequency of free ATP. Furthermore, the time needed to saturate a resonance depends on chemical exchange. If the postulated ATP-INVIS pool exchanged very rapidly with Pi, with a rate constant similar to the rate at which the ATP saturates, then the concentration of saturated ATP would be diluted. In summary, these considerations suggest that an ATP-INVIS pool that saturates relatively slowly or incompletely under the experimental conditions we used is both theoretically possible and consistent with our data and our model.

Structure of the Model and Analysis of Assumptions

The compartmentation model developed here has the following unique characteristics: (a) The model uses data obtained from time-dependent saturation transfer analyses and does not rely on a single measurement made when the magnetization process reaches a steady state. (b) The model uses compartmental theory (which is not the same as the mere assumption that reactants are compartmentalized) to exploit the fact that CrP does not exchange with any other reactant besides ATP. (c) The model treats an assumed invisible and nonsaturable ATP pool in a specific and quantitative fashion. (d) The model accounts for double-exponential behavior sometimes observed in saturation-transfer data. (e) The model provides new and potentially helpful insights concerning the location and magnitude of a sequestered ATP pool and permits analysis of the major phosphate exchange reactions defining high-energy supply in muscle.

The model is based on several assumptions, each of which has limitations. The model assumes that the saturation transfer data (for the $\text{CrP} \rightarrow [\gamma - \text{P}]\text{ATP}$ reaction) cannot always be adequately described by a single exponential. The observation that magnetization transfer data for the creatine kinase reaction requires multiexponential fits is not unprecedented. Gadian et al. (10) observed relaxation for ATP in anaerobic frog muscle that was "not truly exponential." Our results for skeletal muscle show behavior that can be shown statistically to be double-exponential for both the stimulated and unstimulated preparations. The data for the rat heart operating at high workloads also appear to describe a double-exponential decay. In this case it was not possible, however, to obtain enough points on the curve to prove that the difference from a single exponential was statistically significant. The effects of experimental error in the coefficients of the double exponential function (Eq. 9) on the calculated fluxes should be examined.

Our model depends on an externally supplied value of

$T_1(\text{CrP})$, but not on $T_1(\text{ATP})$. The exact values of T_1 for ATP and CrP are still uncertain, with some groups claiming that the value of T_1 varies with workload (9, 10) while others that it does not (4, 6). The compartmentation model yields results that are qualitatively similar for $T_1(\text{CrP})$ ranging from 2.1 to 2.7 s (Table I).

The model also requires an estimate of m , the size of the ATP-INVIS pool. The results do depend on m (Fig. 5), but the conclusions summarized above are true, regardless of the (fixed) value of m that is used. Our choices of m for the examples shown in Tables I and III were based on published estimates that the total adenine nucleotide pool in rat-heart mitochondria is <10% of the whole-heart content (18).

In addition, the results of the calculations are critically dependent on estimates of the rate of ATP production by oxidative phosphorylation and of ATP hydrolysis, as well as on the site of the ATP-INVIS pool. Another source of artifact might arise from the inability of magnetization-transfer methods to detect relatively slow reactions; for example, the ATPase reaction in resting cat biceps.

Our model gives no information on fluxes from ATP to CrP, so it cannot be used to resolve observed discrepancies between the forward and reverse fluxes of the creatine kinase reaction. Similar methods applied to inversion-transfer or double-saturation experiments, however, could be used to calculate the reverse flux.

Creatine Phosphate Shuttle in Heart

The creatine kinase "cycle" or "creatine phosphate shuttle" model for energy transfer in heart postulates (a) that ATP produced by oxidative phosphorylation is the preferred substrate for the mitochondrial creatine kinase reaction, (b) that CrP, as well as ATP, is an energy-transfer molecule, and (c) to complete the cycle, that bound MM-creatine kinase at the myofibril transfers high-energy phosphate from CrP to ATP used for contraction (24). Regulation of this cycle and its relative contribution to energy transfer in the cell remain controversial (24–26). Results of the compartmentation model for the creatine kinase reaction in heart described here support the hypothesis that the creatine kinase system plays a major role in high-energy phosphate transfer in heart. The double-exponential nature of our magnetization transfer data supports the existence of two distinct ATP pools, and the compartmentation model suggests that the ATP-INVIS pool lies partially or completely in mitochondria. If this is the case, flux for the reaction catalyzed by mitochondrial creatine kinase ($\text{ATP-INVIS} \rightarrow \text{CrP}$) is about 5 times higher in hearts working at high workloads compared to the arrested heart (Fig. 8). Thus, over this range of cardiac performance, mitochondrial creatine kinase flux increases fivefold while oxygen consumption increases about sevenfold. This is consistent with functional coupling of the

mitochondrial creatine kinase reaction and ATP synthesis by oxidative phosphorylation proposed previously (4, 24, 25).

Comparison of the Creatine Kinase Reaction in Heart and Skeletal Muscle

The results presented here offer the opportunity to compare the kinetics of the creatine kinase reaction in cardiac and skeletal muscles. The compartmentation model for saturation transfer data for the forward creatine kinase reaction developed here analyzes three reactions. Each changes differently with respect to changes in workload, and some of the changes differ for cardiac and skeletal muscles. Since the saturation transfer data for cardiac and skeletal muscles were treated exactly alike and analyzed using the same model, these differences are inherent in the data and are not created by the modeling. The differences between the responses of heart and skeletal muscle to increased workload are consistent with the predominance of anaerobic metabolism in skeletal muscle and predominance of aerobic metabolism in cardiac muscle.

For both cardiac and skeletal muscles, the cytosolic creatine kinase reaction, $\text{CrP} \rightarrow \text{ATP-VIS}$, increases about fivefold for the changes in workload studied. For both muscles, the magnitude of the flux for the cytosolic reaction, $\text{CrP} \rightarrow \text{ATP-VIS}$, is greater than flux for the (presumed) mitochondrial creatine kinase reaction, $\text{ATP-INVIS} \rightarrow \text{CrP}$. This is consistent with the high ratio of cytosolic vs. mitochondrial creatine kinase activity in both tissues. The ratios of cytosolic to mitochondrial creatine kinase activities in heart and skeletal muscle are 3:1 and 49:1, respectively (unpublished results).

In heart, the mitochondrial creatine kinase reaction $\text{ATP-INVIS} \rightarrow \text{CrP}$ is driven by mitochondrial ATP-INVIS production and increases as much as fivefold as cardiac performance increases while the reverse reaction $\text{CrP} \rightarrow \text{ATP-INVIS}$ is negligible at all workloads. This is predicted from the kinetic properties of the mitochondrial creatine kinase reaction *in vitro* (25). In skeletal muscle, the mitochondrial creatine kinase reaction $\text{ATP-INVIS} \rightarrow \text{CrP}$ increases only slightly while the reverse direction decreases with increased workload. These differences imply that the mitochondrial creatine kinase reaction is more important in the production of high-energy phosphate compounds needed for contraction in heart than in skeletal muscle. This is consistent with the higher tissue content of mitochondrial creatine kinase in heart compared to skeletal muscle (1.6 vs. 0.5 IU/mg protein: unpublished results).

Finally, the total flux from CrP to all forms of ATP is workload independent in skeletal muscle, but is workload-dependent in heart. These results are consistent with the notion that in stimulated skeletal muscle almost all the ATP is generated anaerobically, whereas in heart operating at increasing levels of cardiac performance, ATP is

generated aerobically in mitochondria. In heart, ATP production by oxidative phosphorylation is obligatorily coupled to the mitochondrial creatine kinase reaction.

We thank John Newell for helpful conversations, and Dr. David Stagg for the use of the facilities of the Biomedical Computing Unit at Yale University.

This work was supported by National Institutes of Health grants HL-26215 and HL-28012. John A. Bittl was supported by National Service Research Award HL07049.

Received for publication 25 July 1985 and in final form 11 December 1986.

REFERENCES

1. Jacobus, W. E. and A. Lehninger. 1973. Creatine kinase of rat heart mitochondria. *J. Biol. Chem.* 248:4803-4811.
2. Turner, D. C., T. Wallimann and, E. M. Eppenberger. 1973. A protein that binds specifically to the *m*-line of skeletal muscle is identified as the muscle form of creatine kinase. *Proc. Natl. Acad. Sci. USA.* 70:702-705.
3. Veech, R. L., J. W. R. Lawson, N. W. Cornell, and H. A. Krebs. 1979. Cytosolic phosphorylation potential. *J. Biol. Chem.* 254:6538-6547.
4. Bittl, J. A., and J. S. Ingwall. 1985. Reaction rates of ATP synthesis and creatine kinase in the isolated rat heart: a ^{31}P NMR magnetization transfer study. *J. Biol. Chem.* 260:3512-3517.
5. Kupriyanov, V. V., A. Y. Steinschneider, E. K. Runge, V. T. Kapelko, M. Y. Zueva, V. L. Lakomkin, V. N. Smirnov, and V. A. Saks. 1984. Regulation of energy flux through the creatine kinase reaction *in vitro* and in perfused rat heart: ^{31}P NMR studies. *Biochim. Biophys. Acta.* 805:319-331.
6. Nunnally, R. L., and D. P. Hollis. 1979. Adenosine triphosphate compartmentation in living hearts: a phosphorus nuclear magnetic resonance saturation transfer study. *Biochemistry.* 18:3642.
7. Miceli, M. V., J. A. Hoerter, and W. E. Jacobus. 1983. Evidence supporting the phosphocreatine-ATP energy transport shuttle in perfused rabbit heart: A ^{31}P NMR saturation transfer study. *Circulation.* 68:III-65.
8. Degani, H., M. R. Laughlin, S. L. Campbell, T. Ogino, and R. G. Shulman. 1984. ^{31}P inversion transfer studies of creatine kinase kinetics *in vitro* and in the perfused heart. In Proceedings of the Third Annual Meeting, Society of Magnetic Resonance in Medicine, New York. 185-186.
9. Matthews, P. M., J. L. Bland, D. G. Gadian, and G. K. Radda. 1982. A ^{31}P NMR saturation transfer study of the regulation of creatine kinase in the rat heart. *Biochim. Biophys. Acta.* 721:312-320.
10. Gadian, D. G., G. K. Radda, T. R. Brown, E. M. Chance, M. J. Dawson, and D. R. Wilkie. 1981. The activity of creatine kinase in frog skeletal muscle studied by saturation transfer nuclear magnetic resonance. *Biochem. J.* 194:215-228.
11. Meyer, R. A., M. J. Kushmerick, and T. R. Brown. 1982. Application of ^{31}P NMR spectroscopy to the study of striated muscle metabolism. *Am. J. Physiol.* 242:C1-C11.
12. Forsen, S., and R. Hoffman. 1964. Exchange rates by nuclear magnetic multiple resonance. III. Exchange reactions in systems with several nonequivalent sites. *J. Chem. Phys.* 40:1189.
13. Riggs, D. S. 1963. The mathematical approach to physiological problems. Williams and Wilkins, Baltimore.
14. Kushmerick, M. J. 1983. Energetics of muscle contraction. In Handbook of Physiology, Section 10: Skeletal Muscle. L. D. Peachey, R. H. Adrian and S. R. Geiger, editors. American Physiological Society, Bethesda. 189-236.
15. Sokal, R. R., and F. J. Rohlf. 1969. Biometry. W. H. Freeman, San Francisco. 570.

16. Steele, R. G. D., and H. H. Torrie. 1960. Principles and Procedures of Statistics. McGraw-Hill, New York. 350.
17. Saks, V. A., G. B. Chernousova, D. E. Gukovsky, W. N. Smirnov, and E. I. Chazov. 1975. Studies of energy transport in heart cells. *Eur. J. Biochem.* 57:273-290.
18. Chance, B. 1967. The energy-linked reaction of calcium with mitochondria. *J. Biol. Chem.* 240:2729-2748.
19. LaNoue, K. F., J. Bryla, and J. R. Williamson. 1972. Feedback interactions in the control of citric acid cycle activities in rat heart mitochondria. *J. Biol. Chem.* 247:667-679.
20. LaNoue, K. F., M. Jeffries, and G. K. Radda. 1985. Control of cardiac respiration by reversal of ATP synthesis. *Fed. Proc.* 44:676. (Abstr.)
21. Koretsky, A. P., M. P. Klein, T. L. James and W. M. Weiner. 1984. Investigation of phosphate exchange reactions in kidney and heart *in vivo*. In Proceedings of the Third Annual Meeting, Society of Magnetic Resonance in Medicine, New York. 429-430.
22. Koretsky, A. P., M. P. Klein, T. L. James, and M. W. Weiner. 1984. Quantitation of competing reactions and detection of small metabolite pools using magnetization transfer techniques. In Proceedings of the Third Annual Meeting, Society of Magnetic Resonance in Medicine, New York. 431-432.
23. Balaban, R. S., H. L. Kantor, and J. A. Ferretti. 1983. *In vivo* flux between phosphocreatine and ATP determined by two-dimensional phosphorus NMR. *J. Biol. Chem.* 258:12787-12789.
24. Jacobus, W. E. and J. S. Ingwall, editors. 1980. Heart Creatine Kinase. Williams and Wilkins, Baltimore.
25. Jacobus, W. E. 1985. Respiratory control and the integration of heart high-energy phosphate metabolism by mitochondrial creatine kinase. *Annu. Rev. Physiol.* 47:707-725.
26. Meyer, R. A., H. L. Sweeney, and M. J. Kushmerick. 1984. A simple analysis of the "phosphocreatine shuttle." *Am. J. Physiol.* 246:C365-C377.